

Uroguanylin knockout mice have increased blood pressure and impaired natriuretic response to enteral NaCl load

See the related Commentary beginning on page 1138.

John N. Lorenz,¹ Michelle Nieman,¹ Jenine Sabo,¹ L. Philip Sanford,² Jennifer A. Hawkins,² Noet Elitsur,² Lara R. Gawenis,³ Lane L. Clarke,³ and Mitchell B. Cohen²

¹Department of Molecular and Cellular Physiology, University of Cincinnati and

²Division of Pediatric Gastroenterology, Hepatology and Nutrition, Cincinnati Children's Hospital Research Foundation, Cincinnati, Ohio, USA

³Department of Biomedical Sciences, University of Missouri-Columbia, Columbia, Missouri, USA

Guanylin and uroguanylin, peptides synthesized in the intestine and kidney, have been postulated to have both paracrine and endocrine functions, forming a potential enteric-renal link to coordinate salt ingestion with natriuresis. To explore the *in vivo* role of uroguanylin in the regulation of sodium excretion, we created gene-targeted mice in which uroguanylin gene expression had been ablated. Northern and Western analysis confirmed the absence of uroguanylin message and protein in knockout mice, and cGMP levels were decreased in the mucosa of the small intestine. Using chamber analysis of jejunum revealed that Na⁺/H⁺ exchanger-mediated Na⁺ absorption and tissue conductance was not altered in the knockout animals, but short-circuit current, an index of electrogenic anion secretion, was reduced. Renal clearance measurements showed that uroguanylin deficiency results in impaired ability to excrete an enteral load of NaCl, primarily due to an inappropriate increase in renal Na⁺ reabsorption. Finally, telemetric recordings of blood pressure demonstrated increased mean arterial pressure in uroguanylin knockout animals that was independent of the level of dietary salt intake. Together, these findings establish a role for uroguanylin in an enteric-renal communication axis as well as a fundamental principle of this axis in the maintenance of salt homeostasis *in vivo*.

J. Clin. Invest. 112:1244–1254 (2003). doi:10.1172/JCI200318743.

Introduction

Guanylin (1) and uroguanylin (2), expressed primarily in the mammalian intestine but also in the kidney, were identified because of their homology to the bacterial heat-stable enterotoxin (ST) and their ability to bind to the ST receptor, guanylate cyclase-C (GC-C). ST is a worldwide cause of secretory diarrheal disease, whereas guanylin and uroguanylin are thought to modulate intestinal secretion without causing diarrhea. There is now additional evidence that guanylin and uroguanylin have both local intestinal (paracrine) and endocrine functions, forming a potential enteric-renal link to coordinate salt ingestion with natriuresis (for reviews,

see Forte et al., refs. 3–5). Circumstantial evidence suggests that both peptides, particularly uroguanylin, function as endocrine intestinal natriuretic hormones because (a) both circulate in the bloodstream (6–8); (b) high-salt intake increases uroguanylin and guanylin mRNA (9, 10), as well as urinary excretion of uroguanylin (11); and (c) uroguanylin levels are increased in the circulation of patients with renal disease and congestive heart failure (12, 13). In addition, the cellular localization of uroguanylin in enterocytes of the proximal small intestine is consistent with the luminal and systemic secretion of enteric uroguanylin (11, 14–16). Thus, these peptides may complement the renal effects of the cardiac natriuretic peptides.

If guanylin peptides are to serve as postulated “intestinal natriuretic peptides,” then it should be possible to demonstrate that exogenous administration can induce increases in renal sodium excretion. Indeed, there are reports that guanylin and uroguanylin can initiate diuretic, natriuretic, and kaliuretic responses both *in vivo* and *ex vivo* in rats and mice, with uroguanylin being substantially more potent than guanylin in eliciting these renal effects (17, 18). However, it is important to note that, in the isolated perfused kidney, there was no effect of 190 nM uroguanylin (the lowest dose tested) on urine flow rate and minimal

Received for publication April 24, 2003, and accepted in revised form August 26, 2003.

Address correspondence to: John N. Lorenz, Department of Molecular and Cellular Physiology, University of Cincinnati School of Medicine, 231 Albert Sabin Way, Cincinnati, Ohio 45267-0576, USA. Phone: (513) 558-3097; Fax: (513) 558-5738; E-mail: john.lorenz@uc.edu.

Conflict of interest: The authors have declared that no conflict of interest exists.

Nonstandard abbreviations used: Na⁺-H⁺ exchanger (NHE); heat-stable enterotoxin (ST); guanylate cyclase-C (GC-C); embryonic stem (ES); Krebs-bicarbonate-Ringer solution (KBR); ethyl isopropyl amiloride (EIPA); blood pressure (BP); gastrointestinal (GI); guanylate cyclase-A (GC-A).

effect on fractional sodium reabsorption (17). Similarly, in the intact mouse, natriuretic and diuretic effects were seen at a uroguanylin dose that would be expected to result in plasma concentrations in the nanomolar range (18). Since measured levels of immunoreactive uroguanylin (uroguanylin/prouroguanylin) are 5–7 pM under normal conditions, and moderately higher (<50 pM) in chronic renal disease (11), it remains to be determined whether changes in circulating uroguanylin within the physiologic range can influence renal NaCl excretion in response to changes in dietary salt. Finally, although increases in the urinary excretion and renal expression of uroguanylin have been demonstrated in response to altered dietary NaCl intake (10, 11), no such changes in plasma levels have been documented (19).

Work from several laboratories including ours has shown that uroguanylin, and possibly guanylin, are synthesized within the kidney itself, suggesting that guanylin peptides represent not only an endocrine system, but possibly a local, intrarenal paracrine, and/or autocrine system modulating renal function directly (14, 15, 20). Further evidence for the importance of the guanylin peptides is derived from the observation that the structure of these peptides is highly evolutionarily conserved (21). Thus, to further explore the *in vivo* role of uroguanylin in the regulation of sodium excretion, we created gene-targeted mice in which uroguanylin gene expression has been ablated. The studies reported here present evidence, for the first time, that uroguanylin is a key regulator of renal excretion after ingestion of a dietary salt load and that there is a novel enteric-renal communication axis mediated by uroguanylin.

Methods

Generation of mutant mice. A genomic clone for uroguanylin was isolated by screening a phage library of 129/SvJ genomic DNA using a uroguanylin cDNA probe as previously described (22). A 5.62-kb *EcoRI* fragment of the uroguanylin gene (*Guca1b*) representing –3208 to +2412 was subcloned into pBluescript (SK+) (Stratagene, LaJolla, California, USA). A *HindIII* fragment (–140 to +807) was replaced with a 1.15-kb pMC1neo cassette in the negative orientation. This vector was linearized with *SacII* and electroporated into embryonic stem (ES) cells derived from 129/SvJ mice as previously described (23). Prior to this, the construct was sequenced (University of Cincinnati Sequencing Core) at all ligation junctions to ensure base sequence fidelity. The ES cells were then cultured in the presence of G418. DNA was isolated from cells that survived the selection procedure and analyzed using a PCR screening protocol wherein one primer was outside the targeting vector's sequence homology and the other primer was inside the pMC1neo cassette (see Figure 1). Two correctly targeted clones were identified. Blastocyst-mediated transgenesis was performed into C57BL/6-derived blastocysts that were

implanted into pseudopregnant females. Chimeric mice were bred with Black Swiss mice, and a colony carrying the null allele was established by breeding heterozygous mutant mice onto a Balb/c background. Littermates were used for controls. These studies and the experiments described below were performed in accordance with the guidelines established by the Institutional Animal Care and Use Committee at the University of Cincinnati College of Medicine and Cincinnati Children's Hospital Medical Center.

Genotype analysis. Genomic DNA, digested with *EcoRI* or *MscI*, was analyzed by Southern blot probed with a 405-bp fragment containing genomic DNA from exon 1 representing base pairs +60 to +465 of the mouse uroguanylin coding sequence. Subsequent analyses were performed by PCR with different primers. A 399-bp fragment from the WT gene was amplified using a PCR forward primer (5'-AACCCAGAGGTGTCAGCTTG-3') and a reverse primer (5'-CCTCCAGTGAGCACAAGCT-3'). A 493-bp product from the mutant gene was amplified using primers complementary to the neo^r gene (5'-AAGAACTCGTCAAGAAGGCGATAGAAGGCCG-3') and (5'-AGGATCTCCTGTCATCTCACCTTGCTCCTG-3').

Northern analysis. Animals were killed by CO₂ asphyxiation during a daily 2-hour window to avoid differences in circadian expression of guanylin and uroguanylin. For protein and mRNA studies, the intestine was flushed with cold saline, separated into segments, and stored at –80°C. Intestinal segments were defined as follows: proximal jejunum (proximal third of the small intestine), distal jejunum (middle third of the small intestine), ileum (distal third of the small intestine), cecum, proximal colon (proximal 40% of colon), and distal colon (distal 60% of the colon). Frozen tissue was pulverized, and RNA was extracted using Trizol Reagent (Gibco BRL; Gaithersburg, Maryland, USA) as described previously (16). Portions of the guanylin, uroguanylin, and guanylate cyclase-C cDNAs were radiolabeled with { α -³²P} (DuPont-NEN, Boston, Massachusetts, USA) using the Random Primer Labeling system (Roche Molecular Biochemicals, Indianapolis, Indiana, USA) as described previously (15, 24). Blots were visualized and quantitated using a Molecular Dynamics PhosphorImager system (Molecular Dynamics, Piscataway, New Jersey, USA).

Real-time RT-PCR. Real-time RT-PCR was performed to determine the levels of guanylin, uroguanylin, and GC-C mRNA in kidneys of WT, heterozygote, and null mice. Primer pairs for guanylin were forward (5'-GAG TGA CAT CGC TTG CCT TTC-3') and reverse (5'-TGA GTT TGT TAG CCT CGT GAC TTC-3'); primer pairs for uroguanylin were forward (5'-TGA GTT GGA GGA GAA GGA GAT GTC-3') and reverse (5'-AAG GGC AAG GCT GGG TTA TG-3'); and primer pairs for GC-C were forward (5'-CGG ATT GTC AGT TCC TGT ATG AAG-3') and reverse (5'-GCC AGT ATG TGG TTT CTG TCC C-3'). Real-time RT-PCR was performed on an Mx4000 Multiplex Quantitative PCR System (Stratagene, La Jolla, California, USA). Detection of

the PCR product was performed using SYBR-Green (Stratagene) and normalized to glyceraldehyde-3-phosphate dehydrogenase expression.

Western analysis. Animals were killed, and tissues were collected as described above. Tissue was homogenized and processed as described previously (16). Membranes were immunoblotted using a 1:1000 dilution of antisera that recognizes proguanylin (antibody 2538) and prouroguanylin (antibody 6910) (16). These antibodies were generously provided by Michael Goy of the University of North Carolina at Chapel Hill and have been previously validated and described (25, 26). Following incubation with a horseradish peroxidase-conjugated secondary antibody, the signal was visualized on Kodak X-OMAT AR film (Eastman Kodak Co., Rochester, New York, USA) using a commercially available chemiluminescent kit (Perkin Elmer Life Sciences, Boston, Massachusetts, USA). As a control for loading, blots were reevaluated with an actin probe (gift of J.L. Lessard, Cincinnati Children's Hospital Research Foundation).

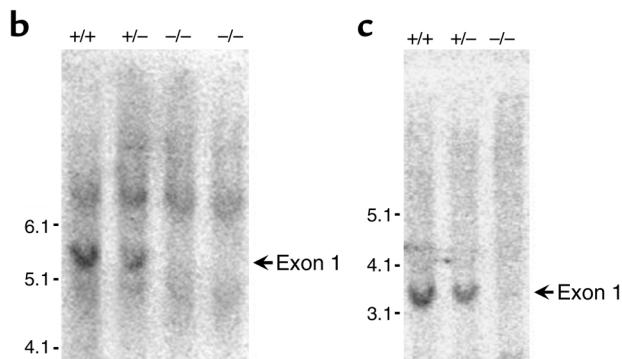
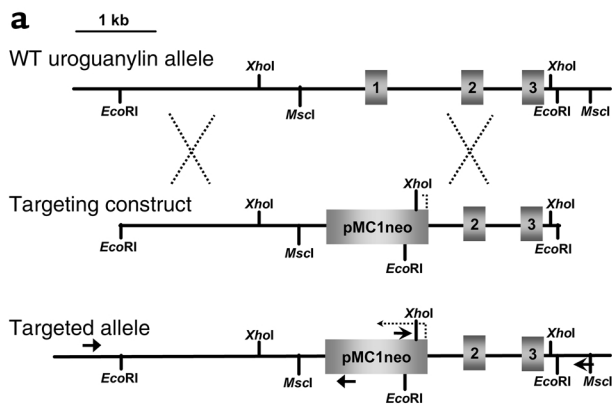
cGMP measurements. The proximal jejunum, ileum, and colon were dissected and flushed with PBS and laid flat using a lengthwise incision. A glass slide was used to scrape the mucosal surface of these segments, and the scrapings were immediately placed in liquid nitrogen. The tissue was homogenized in 6% trichloroacetic acid to give a 10% w/v homogenate. The homogenate was washed five times with 4 volumes of water-saturated diethyl ether, dried under nitrogen for 30 minutes, and resuspended in 0.05 M sodium acetate, pH 6.2. cGMP was then measured in a validated radioimmunoassay, and cGMP extractions were normalized per microgram of tissue wet weight (27).

In vitro jejunal flux measurements. Animals were killed by asphyxiation in 100% CO₂, and approximately 5 cm of proximal jejunum were removed and placed in oxygenated, ice-cold Ringer solution, opened along the mesenteric border, and divided into sections (smooth muscle intact) for mounting in standard Ussing chambers (0.238-cm² exposed surface area). The mucosal and serosal surfaces were independently bathed with a Krebs-bicarbonate-Ringer solution (KBR) with the following composition (in mM): 115 NaCl, 25 NaHCO₃, 2.4 KH₂PO₄, 0.4 K₂HPO₄, 1.2 MgCl₂, and 1.2 CaCl₂, pH 7.4. Glucose (10 mM) was added to the serosal bath, and mannitol (10 mM) was added to the mucosal bath to avoid currents due to Na⁺-coupled glucose cotransport (28). Bathing solutions were gassed with 95% O₂ and 5% CO₂ using a gas-lift recirculation system and warmed to 37°C. Indomethacin (1 μM) was added to the KBR solution for both tissue dissection and experiments to minimize exposure to endogenously generated prostanoids (29). After mounting, tetrodotoxin (0.1 μM) was added to the serosal bath to minimize variation in the intrinsic neural tone (29), and sections were allowed to equilibrate to a steady-state level for a minimum of 30 minutes before beginning each experiment.

Transepithelial short-circuit current (I_{sc}) was measured in jejunal segments from uroguanylin knockout ($Ugn^{-/-}$, $n = 9$) and WT mice ($Ugn^{+/+}$, $n = 9$) via an automatic voltage clamp (VCC-600, Physiologic Instruments, San Diego, California, USA), as previously described (29). Experiments were performed under short-circuited conditions with the serosal bath as a ground. At 5-minute intervals, tissue conductance (G_t) was calculated using Ohm's law by applying a 5-mV pulse and measuring the resulting current deflection. For unidirectional mucosal-to-serosal Na⁺ flux (J_{ms}) measurements, ²²Na (2 μCi, Amersham Life Science, Arlington Heights, Illinois, USA) was added to the mucosal bath, and serosal ²²Na accumulation was determined from triplicate aliquots (250 μl) from the serosal bath at the beginning and end of each flux period (29). ²²Na flux was determined in separate tissues, paired by G_t , in the presence and absence of *N*-ethyl-*N*-isopropyl-amiloride (EIPA, 100 μM in DMSO; RBI, Natick, Massachusetts, USA), and the difference (EIPA-sensitive flux) was considered a measure of Na-H exchange activity (30, 31). Samples were analyzed by counting for 5 min in a gamma radiation counter (Packard Instruments, Meriden, Connecticut, USA).

Renal function measurements. Male mice, 15 to 23 weeks old, were fasted overnight and prepared for clearance measurements as previously described (32). Briefly, mice were anesthetized with ketamine (50 μg/g body weight, i.p.) and thiobutobarbital (Inactin, 100 μg/g body weight i.p., Sigma-Aldrich, St. Louis, Missouri, USA), and placed on a temperature-controlled table. Following tracheotomy, the right femoral artery and vein were cannulated for the measurement of arterial pressure and the administration of maintenance solutions. Arterial pressure was monitored using an Argon model CDXIII transducer (Maxxim Medical, Clearwater, Florida, USA) connected to a PowerLab data acquisition system (AD Instruments, Colorado Springs, Colorado, USA). The bladder was cannulated for the collection of urine. A 3-μl/g body weight bolus of 1% FITC-insulin (Sigma-Aldrich) in isotonic saline was administered, followed by a maintenance infusion of the same solution at 0.15 μl/min/g body weight, and the animals were allowed to equilibrate for 30 minutes.

Enteral sodium loading. $Ugn^{-/-}$ ($n = 7$) and $Ugn^{+/+}$ mice ($n = 6$) were further prepared for gastric gavage by inserting PE-50 tubing orally into the esophagus, advancing into the stomach, and securing with a 5-0 silk ligature. Following equilibration, a 30-minute control urine collection was made with an 80-μl blood sample at the midpoint. This and all subsequent blood samples were replaced with an equal volume of whole blood from a donor animal. Upon completion of the control period, 1.0 ml of 300 mM NaCl was delivered through the gastric catheter over 2 to 3 minutes. Immediately following, five additional clearance periods were performed (20, 20, 20, 30, and 30 minutes in duration) in the same manner as the control period in order to follow the time course of excretion of the NaCl load.



Intravenous sodium loading. $Ugn^{-/-}$ ($n = 5$) and $Ugn^{+/+}$ mice ($n = 5$) were instrumented with a second venous catheter for intravenous infusion of NaCl. Following an initial control period as described above, animals were given a 1.0-ml intravenous bolus infusion of 300 mM NaCl, over a 2- to 3-minute period. Immediately following, five additional clearance periods were performed exactly as described above.

Telemetric recording of blood pressure. Continuous ambulatory blood pressure (BP) recordings were made using the TA11PA-C20 pressure transmitter

Figure 1

(a) Targeting scheme used to disrupt the uroguanylin locus. Recombination between the targeting vector and the WT allele produced the targeted allele where 140 bp of the promoter and 807 bp of the uroguanylin gene including exon 1 are replaced by a PMC1neo polyA⁺ cassette. The arrow above the neo cassette indicates the direction of transcription. The two pairs of arrows represent the approximate locations of PCR primers used to identify targeted ES cell clones. Separate primer pairs were used for PCR genotype as indicated in the text. (b) Southern blot of genomic DNA digested with *EcoRI*; (c) Southern blot digested with *MscI*. These blots were probed with a 405-bp fragment containing genomic DNA from exon 1, representing base pairs +60 to +465 of the mouse uroguanylin coding sequence. The loss of the WT allele is seen in the null animals only.

(Data Sciences International, St. Paul, Minnesota, USA). Each transmitter was calibrated prior to implantation by applying known pressure steps to the transducer and recording the output. The output signal from each Model RPC-1 receiver was channeled to a R11CPA Pressure Analog Adaptor, and recorded and analyzed using a PowerLab system. Transmitters were implanted using carotid artery cannulation and subcutaneous transmitter placement under isoflurane anesthesia as described (33). Following implantation, $Ugn^{-/-}$ ($n = 5$) and $Ugn^{+/+}$ mice ($n = 6$) were returned to their home cages for monitoring and allowed to recover prior to data collection. The mice were synchronized to a 12:12-hour light-dark schedule with lights on at 7:00 A.M. Thereafter, mice were maintained on either low (0.01% NaCl), normal (1% NaCl) or high (5% NaCl) salt diets, and BP monitored in 1-minute episodes at 5-minute intervals.

Statistics. Statistical analysis was performed by ANOVA using a single-factor design or a mixed factorial design with repeated measures on the second factor. Where necessary, individual comparisons were accomplished using individual contrasts. Data are expressed as means \pm SEM, and differences are regarded as significant at $P < 0.05$.

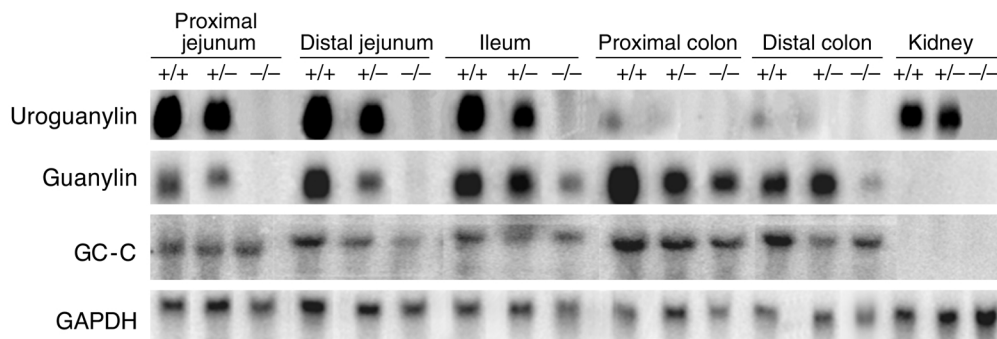


Figure 2

Northern analysis of uroguanylin WT, heterozygous, and null mice. A portion of the uroguanylin, guanylin, and GC-C cDNA was used as a probe on Northern blots of proximal jejunum, distal jejunum, ileum, proximal colon, distal colon, and kidney. Uroguanylin mRNA is more prominently expressed in the small intestine and kidney. Levels of uroguanylin mRNA were reduced in heterozygotes and absent in null mice. Guanylin mRNA is expressed more prominently in distal small intestine and colon. Levels of guanylin mRNA were also reduced in uroguanylin heterozygous and null animals. Levels of GC-C appear to be similar across different intestinal segments and genotypes. GAPDH expression is shown as a loading control.

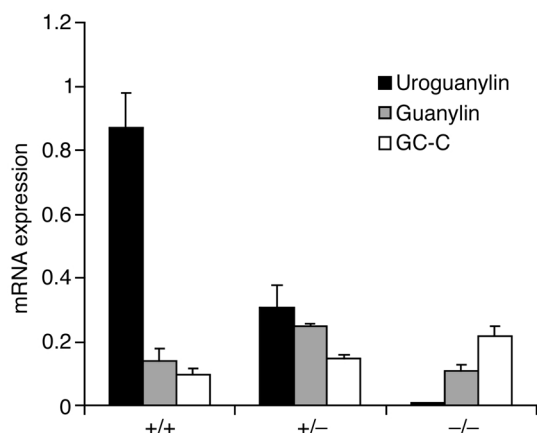


Figure 3

Real time RT-PCR of renal tissue from uroguanylin WT, heterozygous, and null mice. Uroguanylin mRNA is reduced in heterozygote and absent in null mice. Guanylin mRNA is present at low levels and is not significantly different between the three genotypes. GC-C mRNA is present at low levels but increases in guanylin-deficient mice ($P = 0.05$).

Results

Generation of *Ugn*^{-/-} mice. Following gene targeting of the uroguanylin allele, as illustrated in Figure 1a, Southern blots were used to confirm the generation of heterozygous (+/-) and knockout (-/-) animals (Figure 1, b and c). *Ugn*^{-/-} mice grew normally to adulthood and were of similar weight as WT controls. Initial morphological evaluation of these mice using hematoxylin and eosin staining revealed a normal crypt-villus structure (data not shown).

Northern, real-time RT-PCR, and Western analysis of *Ugn*^{-/-} mice. In order to confirm inactivation of the uroguanylin gene, we compared expression of uroguanylin mRNA and protein in *Ugn*^{-/-} mice with that in *Ugn*^{+/+} and *Ugn*^{+/-} mice. By Northern analysis, no uroguanylin signal was found in uroguanylin null mice, and the signal was reduced in the proximal jejunum, distal jejunum, ileum, and kidney of heterozygous mice (Figure 2). The guanylin and uroguanylin genes are located extremely close to each other at both mouse and human chromosomal loci (intragenic gap approximately 7 kb), and their mRNA expression patterns and functional similarity suggests coordinate regulation in a manner that allows for the presence of a binding ligand in all regions of the intestinal tract (15, 22, 34). Although the guanylin gene was not disrupted by the uroguanylin targeting process (Southern blot not shown), we found that the Northern blot guanylin signal was reduced in the small and large intestine of uroguanylin heterozygous and null animals (Figure 2). In contrast, there appeared to be no change in the mRNA levels for the uroguanylin receptor, GC-C (Figure 2). Real-time PCR determination of mRNA levels in mouse kidney demonstrated significantly reduced uroguanylin mRNA in the *Ugn*^{+/-} mice and none in *Ugn*^{-/-} (Figure 3). Levels of guanylin appeared unchanged in the *Ugn*^{+/-} and *Ugn*^{-/-} mice, whereas levels of GC-C were increased in the uroguanylin deficient mice ($P = 0.05$).

Western analysis of intestinal tissue from uroguanylin null mice was performed to confirm the loss of uroguanylin prohormone. We used antisera that recognized the prohormone portion of the uroguanylin protein and found no traces of prouroguanylin in the proximal jejunum, ileum, and proximal colon of *Ugn*^{-/-} mice (Figure 4, top). Levels of prouroguanylin were reduced in proximal jejunum and ileum in heterozygous mice. In addition, using antisera for guanylin prohormone, we found that the cellular level of proguanylin protein was significantly reduced in *Ugn*^{-/-} mice. These data indicate that loss of the uroguanylin gene and activity can affect the levels of guanylin expression in enterocytes, although further studies will be needed to confirm that levels of guanylin secretion into the intestine are altered in uroguanylin null mice.

cGMP levels in *Ugn*^{-/-} mice. GC-C is the major transmembrane guanylate cyclase in the intestine and the only known endogenous ligands of GC-C are guanylin and uroguanylin. Loss of uroguanylin might be expected to result in diminished cGMP levels in regions of the intestine that do not have appreciable levels of guanylin. Accordingly, we found that cGMP content in mucosal scrapings from proximal jejunum and ileum of *Ugn*^{-/-} mice was significantly less than *Ugn*^{+/+} littermates, whereas colonic cGMP was similar in both groups (Figure 5). Normally, uroguanylin expression is robust in the small intestine, and guanylin expression is highest in the large intestine. Although there appears to be significant loss of guanylin in the uroguanylin knockout colon, the remaining guanylin may be sufficient to maintain normal levels of cGMP.

Jejunal flux measurements in *Ugn*^{-/-} mice. EIPA-sensitive, unidirectional sodium flux (mucosal to serosal), used as a measure of Na⁺ absorption via Na-H exchange, was not different between *Ugn*^{-/-} and *Ugn*^{+/+} mice as shown in Figure 6a. Similarly, total tissue conductance, G_t , was not different between the two groups of animals, under either control conditions (DMSO vehicle), or during EIPA treatment (Figure 6b). In contrast, short-circuit current (I_{sc}), which is generally reflective of anion secretion in the jejunum, is significantly reduced in *Ugn*^{-/-} mice, compared with *Ugn*^{+/+} in the presence or absence of EIPA (Figure 6c). I_{sc} was essentially not different from zero in the UGN-deficient tissues.

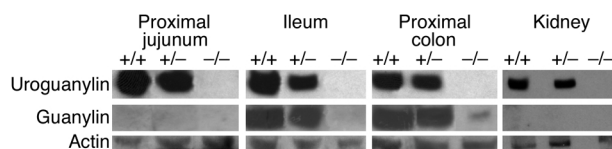


Figure 4

Western analysis of uroguanylin WT, heterozygous, and null mice. Uroguanylin prohormone is reduced in heterozygous mice and absent in null mice. Guanylin prohormone is also reduced in uroguanylin heterozygous mice and severely reduced or absent in uroguanylin null mice. Results from an actin probe are shown as a loading control.

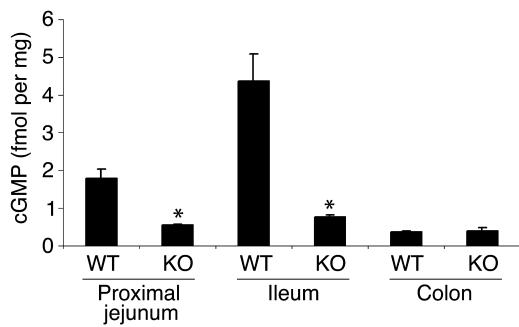


Figure 5

cGMP levels in epithelia from the proximal jejunum, ileum, and colon. Levels of cGMP were approximately 2.5-fold higher in the proximal jejunum and more than 5-fold higher in ileum in WT animals compared with uroganylin knockout animals. Levels of cGMP were similar in WT and knockout colon. $n = 4$ to 5-fold per segment. * $P < 0.001$.

Baseline renal function in $Ugn^{-/-}$ mice. Body weights and kidney weights were not different between any of the four groups and averaged 34 ± 2 g and 0.491 ± 0.016 g for $Ugn^{+/+}$ enteral-loaded; 33 ± 1 g and 0.488 ± 0.022 g for the $Ugn^{-/-}$ enteral-loaded; 33 ± 2 and 0.499 ± 0.045 g for the $Ugn^{+/+}$ i.v.-loaded; 38 ± 3 g and 0.484 ± 0.022 g for the $Ugn^{-/-}$ i.v. loaded. For initial statistical analysis, baseline data from the two loading protocols (enteral and i.v.) were combined within the genotype groups since animals were treated the same prior to NaCl loading. As shown in Tables 1 and 2, under baseline conditions there were no significant differences in BP, plasma potassium concentration (P_K), GFR, or filtered load of Na^+ (FL Na^+ , Figure 7 at time 0), between $Ugn^{-/-}$ or $Ugn^{+/+}$ animals. However, plasma Na^+ concentration (P_{Na}) was significantly higher, and Na^+ , K^+ and fluid excretion were all significantly lower in $Ugn^{-/-}$ compared with $Ugn^{+/+}$ animals under baseline conditions. Other renal function variables were not different under baseline conditions between the two groups.

Response to enteral NaCl loading in $Ugn^{-/-}$ and $Ugn^{+/+}$ mice. In response to enteral NaCl loading, there were no differences in the response of BP, P_{Na} and P_K between $Ugn^{-/-}$ and $Ugn^{+/+}$ mice (Table 1). It should be

noted, however, that P_{Na} increased similarly in both groups in response to enteral NaCl loading such that it remained higher in the UGN-KO mice compared with WT throughout the experiment. Hematocrit was not different and decreased comparably in the two groups of mice in response to enteral NaCl loading, indicating equal degrees of extracellular volume distribution in the two genotypes (data not shown). As shown in Figure 7a, the filtered load of Na^+ increased initially in the KO mice in response to enteral loading and reached a peak during the 20- to 40-minute period, and thereafter declined to a value not different from baseline by the end of the experiment. In contrast, the Na^+ filtered load did not change initially in the WT mice in response to enteral NaCl loading, but in the final clearance period (90–120 minutes) declined to a level that was significantly lower than baseline. These observed changes in Na^+ filtered load were primarily due to a similar pattern of changes in GFR (Table 1). Na^+ excretion rate increased in response to enteral NaCl in both $Ugn^{-/-}$ and $Ugn^{+/+}$ mice, such that it remained at lower levels in the knockout mice throughout the experiment. When expressed in terms of cumulative excretion of the applied NaCl load, as shown in Figure 7b, there was a significant interaction between the amount of Na^+ excreted over time in the $Ugn^{-/-}$ versus the $Ugn^{+/+}$ mice, such that even by the 20- to 40-minute time period there was significantly less of the Na^+ load excreted in $Ugn^{-/-}$ animals compared with $Ugn^{+/+}$. These changes were primarily related to an increase in tubular Na^+ reabsorption in the $Ugn^{-/-}$ mice during the initial 60 minutes following the NaCl load, whereas it remained unchanged in the $Ugn^{+/+}$ animals for the entire 120-minute period following NaCl (Table 1). K^+ excretion in $Ugn^{-/-}$ animals was initially lower compared with $Ugn^{+/+}$, and in response to enteral NaCl it did not decrease to the extent seen in the $Ugn^{+/+}$ mice (Table 1). Again, this difference appears to have been primarily related to increases in tubular K^+ reabsorption, although there were no statistical differences between the two groups. Finally, although there was a significant diuresis in both groups of mice

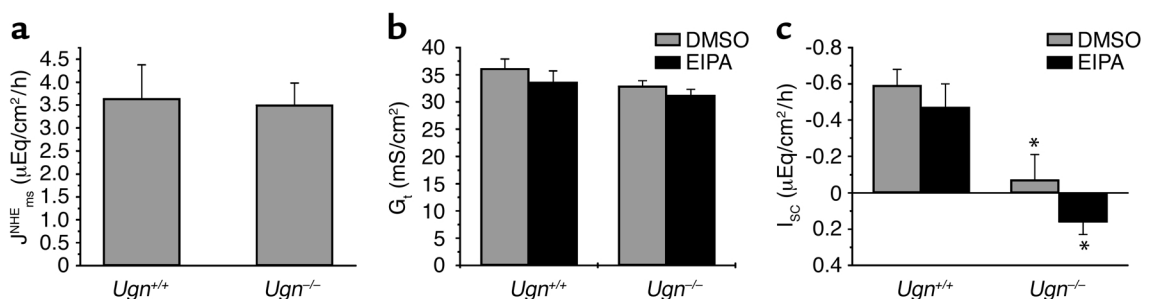


Figure 6

Using chamber bioelectric parameters and flux measurements from jejunal segments from $Ugn^{+/+}$ and $Ugn^{-/-}$ mice ($n = 9$ for each data pair). (a) EIPA-sensitive mucosal-to-serosal Na^+ flux used as an estimate of Na-H exchange-mediated flux (J_m^{NHE}). Individual data points were obtained from separate preparations in the presence and absence of EIPA and paired by G_t . (b) Transepithelial tissue conductance (G_t) in the absence (gray bars) and presence (black bars) of EIPA. (c) Short-circuit current (I_{sc}) in the absence (gray bars) and presence (black bars) of EIPA. * $P < 0.05$ compared with $Ugn^{+/+}$.

Table 1
Hemodynamic and renal response to enteral NaCl loading

		Control	0–20 min	20–40 min	40–60 min	60–90 min	90–120 min
BP	WT	87 ± 6	93 ± 7	103 ± 3 ^A	104 ± 4 ^A	102 ± 6 ^A	101 ± 7
(mmHg)	KO	92 ± 6	95 ± 5	98 ± 4 ^A	97 ± 6 ^A	97 ± 7 ^A	91 ± 8
Hct	WT	53 ± 1	52 ± 1	50 ± 1 ^A	50 ± 2 ^A	50 ± 2 ^A	51 ± 2
(%)	KO	51 ± 1	50 ± 1	48 ± 1 ^A	47 ± 1 ^A	47 ± 1 ^A	47 ± 1 ^A
P _{Na}	WT	159 ± 2	166 ± 2 ^A	166 ± 2 ^A	166 ± 2 ^A	165 ± 2 ^A	165 ± 1 ^A
(mEq/l)	KO ^B	163 ± 1 ^C	171 ± 2 ^{A,C}	170 ± 1 ^{A,C}	171 ± 1 ^{A,C}	171 ± 2 ^{A,C}	171 ± 2 ^{A,C}
P _K	WT	4.13 ± 0.09	3.70 ± 0.11	3.91 ± 0.14	4.09 ± 0.23	4.08 ± 0.16	4.09 ± 0.11
(mEq/l)	KO	4.03 ± 0.16	3.79 ± 0.15	3.86 ± 0.1	4.08 ± 0.14	4.35 ± 0.14	4.78 ± 0.58
GFR	WT	471 ± 57	484 ± 69	460 ± 51	453 ± 47	455 ± 44	392 ± 27 ^A
(μl/min)	KO	441 ± 46	500 ± 76	540 ± 75 ^A	493 ± 55	476 ± 55	441 ± 57
Na ⁺ excretion	WT	0.84 ± 0.21	1.24 ± 0.23 ^A	2.22 ± 0.18 ^A	2.53 ± 0.22 ^A	2.37 ± 0.27 ^A	2.07 ± 0.22 ^A
(μEq/min)	KO ^B	0.50 ± 0.10 ^C	0.95 ± 0.24 ^{A,C}	1.66 ± 0.19 ^{A,C}	1.78 ± 0.23 ^{A,C}	1.67 ± 0.30 ^{A,C}	1.30 ± 0.26 ^{A,C}
Na ⁺ reabsorption	WT	74.0 ± 9.5	78.9 ± 11.0	74.1 ± 8.4	72.3 ± 7.3	72.7 ± 7.2	62.5 ± 4.6
(μEq/min)	KO	71.0 ± 7.4	84.0 ± 12.5 ^A	90.1 ± 12.6 ^A	82.5 ± 9.2 ^A	79.4 ± 8.8	73.4 ± 9.1
K ⁺ excretion	WT	0.70 ± 0.04	0.58 ± 0.03	0.47 ± 0.05	0.48 ± 0.06	0.45 ± 0.04 ^A	0.46 ± 0.04 ^A
(μEq/min)	KO ^B	0.56 ± 0.03 ^C	0.57 ± 0.05	0.46 ± 0.07 ^A	0.47 ± 0.05 ^A	0.51 ± 0.06	0.51 ± 0.05
K ⁺ reabsorption	WT	1.17 ± 0.21	1.14 ± 0.19	1.29 ± 0.17 ^A	1.33 ± 0.15 ^A	1.36 ± 0.15 ^A	1.12 ± 0.11
(μEq/min)	KO	1.12 ± 0.24	1.27 ± 0.33	1.60 ± 0.36 ^A	1.55 ± 0.29 ^A	1.56 ± 0.26 ^A	1.57 ± 0.33
Urine flow	WT	3.4 ± 0.6	3.9 ± 0.5	6.5 ± 0.8 ^A	7.5 ± 0.7 ^A	7.3 ± 0.8 ^A	6.6 ± 0.9 ^A
(μl/min)	KO ^B	2.3 ± 0.3 ^C	3.2 ± 0.5 ^C	4.6 ± 0.5 ^{A,C}	5.1 ± 0.8 ^{A,C}	5.2 ± 1.1 ^{A,C}	4.2 ± 0.9 ^{A,C}
Fluid reabsorption	WT	467 ± 57	480 ± 69	454 ± 52	446 ± 47	448 ± 45	385 ± 28
(μl/min)	KO	438 ± 46	497 ± 76	536 ± 75	488 ± 55	471 ± 55	436 ± 56

WT, *n* = 6; KO, uroguanylin knockout, *n* = 7; BP, mean arterial blood pressure; Hct: hematocrit; P_{Na} and P_K: plasma Na⁺ and K⁺ concentration; GFR: glomerular filtration rate. Values are mean ± SEM. ^A*P* < 0.05 compared with the control value in the same group. ^B*P* < 0.05 compared with WT for pooled control data from enteral- and i.v.-loaded animals (see Table 2). ^C*P* < 0.05 compared with the corresponding time point in the WT group.

following NaCl, the response was such that the urine flow remained lower in the *Ugn*^{-/-} animals compared with *Ugn*^{+/-} throughout the experiment, and total tubular fluid reabsorption did not change in either of the groups (Table 1).

Response to intravenous NaCl loading in *Ugn*^{-/-} mice. In order to determine whether the observed differences in Na⁺ handling between the *Ugn*^{-/-} and *Ugn*^{+/-} animals were specific for gastrointestinal administration of the NaCl load, we performed a series of control experiments to examine the natriuretic response to intravenously delivered NaCl. As in the enteral-loaded animals, there were no substantial differences in the response to i.v. NaCl of BP, P_{Na} and P_K between *Ugn*^{-/-} and *Ugn*^{+/-} mice (Table 2), and again there were no differences in hematocrit between the genotypes. Furthermore, as seen in the previous protocol, P_{Na} increased similarly in both groups of animals, such that the observed elevation in P_{Na} in *Ugn*^{-/-} animals persisted throughout the experiment. Unlike the enteral-loaded animals, however, there were no differences in the response to i.v. NaCl loading between *Ugn*^{-/-} and *Ugn*^{+/-} animals in GFR, filtered Na⁺ load, or Na⁺ excretion rate (Table 2 and Figure 7a). Whereas GFR and filtered Na⁺ were unaffected by i.v. NaCl loading in both groups of animals, Na⁺ excretion increased transiently and equally in both groups. Importantly, the cumulative amount of Na⁺ excreted over the course of the i.v.-loading experiment was excretion nearly identical between the *Ugn*^{-/-} and *Ugn*^{+/-} mice (Figure 7b).

Furthermore, post-hoc analysis indicated that the amount of Na⁺ excreted after 120 minutes in the enteral-loaded *Ugn*^{+/-} animals was not different from the total amount excreted in either of the i.v. loaded groups, whereas the amount excreted after 120 minutes in the enteral-loaded *Ugn*^{-/-} animals was substantially less. There were no differences in tubular Na⁺ reabsorption between the two groups. In response to i.v. NaCl loading, K⁺ excretion decreased more in *Ugn*^{-/-} than *Ugn*^{+/-} mice, but there were no other differences in K or fluid handling.

Telemetric measurement of BP in *Ugn*^{-/-} mice. After telemeter implantation, animals were returned to their home cages for recovery and maintained on the 1% NaCl diet; BP, and heart rate were monitored continuously, and diurnal rhythms were reestablished within 5 to 7 days of surgery. At that time, the 1% NaCl diet was continued for 3 additional days and pressure recorded. Animals were then placed on Na⁺-deficient diet (0.01%) for 3 days, and then on a high-Na⁺ diet (5%) for 3 days, with continuous recording. Figure 8 shows the average BP in *Ugn*^{-/-} and *Ugn*^{+/-} after 3 days on each diet. Values represent average of continuous measurements taken over a 2-hour period (4:00 am–6:00 am) while the animals were resting quietly (as determined from the stability of the BP tracing). Regardless of diet, *Ugn*^{-/-} mice had a significantly higher BP than *Ugn*^{+/-} mice (*P* < 0.02). In both genotypes, average BP was slightly but significantly lower while on the Na-deficient diet compared with both normal

and high-salt diets, which were not different from each other. Importantly, there was no statistical interaction between genotype and diet ($P = 0.47$), indicating that *Ugn*^{-/-} mice were no more salt sensitive than the *Ugn*^{+/+} mice. Measurements taken in the late afternoon (4:00 pm–6:00 pm), when animals were more active, showed a similar pattern of results, but the genotype difference did not reach significance ($P = 0.12$). Finally, we analyzed the acute effect on BP of changing from a 0.01% to 5% NaCl diet. In the 24 hours immediately following the switch, there was no difference in the BP response between the two genotypes (data not shown).

Discussion

The existence of an intestinal natriuretic hormone that delivers a signal from the gastrointestinal (GI)-tract to the kidney in response to increased NaCl intake has been hypothesized since Carey and coworkers showed, in both humans and rabbits, that oral administration of an NaCl load resulted in a greater natriuretic response than the same load given intravenously (35, 36). More recently, studies exploring the physiological effects of guanylin and particularly uroguanylin have identified these gastrointestinal peptides as potential candidates involved in a GI-renal endocrine axis (3). Uroguanylin has an evolutionary role in salt homeostasis dating back to the teleosts, and it is likely that this role has been retained by all other vertebrates that came later (37). Recent work has amplified the role for this hormone family as osmoregulator agents in the intestine and kidney of eels (21). Although there are a

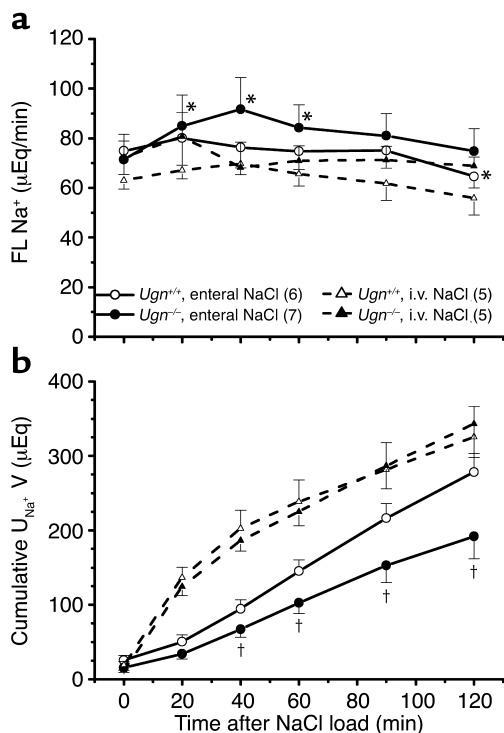
number of experimental observations supporting a role for uroguanylin in regulating renal function in mammals, there are several crucial elements that have thus far eluded investigators. First, in vivo and ex vivo studies have only been able to demonstrate an effect of exogenous uroguanylin on renal excretory function at pharmacologic doses, far exceeding levels found in plasma (17, 18). Second, although plasma uroguanylin levels have been found to change in various pathologic conditions, it has not yet been demonstrated that changes in NaCl intake result in concomitant changes in circulating uroguanylin levels (4, 19, 38). Therefore, in the present study using mice genetically deficient for the uroguanylin gene, we sought to explore whether the natriuretic response to enteral NaCl load was altered in the absence of uroguanylin. Our findings demonstrate a blunted natriuresis following enteral, but not i.v. NaCl loading in uroguanylin-deficient mice. These data, combined with the observation that arterial BP measured by telemetry is elevated in mice lacking uroguanylin, provide evidence for the first time that uroguanylin plays a significant physiologic role in regulating Na⁺ excretion from the kidney in addition to its likely role as a regulator of intestinal secretion.

One of the central findings in the present study was that within 2 hours of the enteral salt load, WT animals had excreted approximately 85% of the administered load, whereas uroguanylin-deficient animals had excreted less than 60%. This impairment appears to be due to an inappropriate increase in tubular Na⁺ reabsorption in null animals that does not occur in WT animals follow-

Table 2
Hemodynamic and renal response to i.v. NaCl loading

		Control	0–20 min	20–40 min	40–60 min	60–90 min	90–120 min
BP (MmHg)	WT	102 ± 7	109 ± 8 ^A	107 ± 8 ^A	107 ± 8 ^A	106 ± 5 ^A	103 ± 6
	KO	101 ± 5	112 ± 5 ^A	113 ± 6 ^A	115 ± 5 ^A	113 ± 5 ^A	108 ± 5
Hct (%)	WT	49 ± 1	45 ± 2 ^A	47 ± 3 ^A	47 ± 3 ^A	48 ± 3	48 ± 4
	KO	51 ± 1	46 ± 1 ^A	49 ± 1 ^A	50 ± 1	51 ± 1	50 ± 2
P _{Na} (mEq/l)	WT	160 ± 1	165 ± 2 ^A	164 ± 3 ^A	163 ± 3 ^A	164 ± 3 ^A	164 ± 3 ^A
	KO ^B	163 ± 1 ^C	168 ± 2 ^{A,C}	168 ± 2 ^{A,C}	167 ± 2 ^{A,C}	167 ± 2 ^{A,C}	168 ± 2 ^{A,C}
P _K (mEq/l)	WT	4.10 ± 0.29	3.60 ± 0.24 ^A	4.08 ± 0.24	3.73 ± 0.08	4.01 ± 0.23	4.13 ± 0.22
	KO	3.62 ± 0.07	3.44 ± 0.10	4.11 ± 0.27 ^A	3.94 ± 0.11	3.88 ± 0.08	3.86 ± 0.14
GFR (μl/min)	WT	394 ± 24	408 ± 20	426 ± 30	404 ± 29	376 ± 40	341 ± 40
	KO	444 ± 57	484 ± 62	407 ± 64	426 ± 36	428 ± 32	410 ± 19
Na ⁺ excretion (μEq/min)	WT	0.64 ± 0.15	5.86 ± 0.58 ^A	3.30 ± 0.59 ^A	1.79 ± 0.35 ^A	1.45 ± 0.32 ^A	1.44 ± 0.34 ^A
	KO ^B	0.41 ± 0.10 ^C	5.60 ± 0.57 ^A	3.11 ± 0.22 ^A	1.93 ± 0.26 ^A	2.06 ± 0.50 ^A	1.88 ± 0.49 ^A
Na ⁺ reabsorption (μEq/min)	WT	62.4 ± 3.5	61.3 ± 4.1	66.5 ± 4.7	63.9 ± 4.8	60.3 ± 6.8	54.5 ± 6.9
	KO	71.9 ± 9.3	75.2 ± 9.3	65.1 ± 10.1	69.1 ± 5.9	69.3 ± 5.5	66.9 ± 3.8
K ⁺ excretion (μEq/min)	WT	0.75 ± 0.06	0.48 ± 0.09 ^A	0.48 ± 0.16 ^A	0.50 ± 0.12 ^A	0.47 ± 0.09 ^A	0.44 ± 0.08 ^A
	KO ^B	0.65 ± 0.08	0.42 ± 0.07 ^A	0.24 ± 0.08 ^{A,C}	0.36 ± 0.06 ^A	0.43 ± 0.02 ^A	0.43 ± 0.04 ^A
K ⁺ reabsorption (μEq/min)	WT	0.85 ± 0.11	1.00 ± 0.12	1.26 ± 0.11 ^A	1.03 ± 0.08 ^A	1.06 ± 0.19	0.98 ± 0.21
	KO	0.96 ± 0.19	1.25 ± 0.27	1.37 ± 0.15 ^A	1.31 ± 0.14 ^A	1.23 ± 0.1	1.15 ± 0.03
Urine flow (μl/min)	WT	2.9 ± 0.4	22.3 ± 2.6 ^A	10.0 ± 2.0 ^A	5.6 ± 1.3 ^A	4.8 ± 1.0 ^A	5.0 ± 1.1 ^A
	KO ^B	1.7 ± 0.1 ^C	21.7 ± 3.4 ^A	9.5 ± 1.0 ^A	5.4 ± 0.9 ^A	6.6 ± 1.8 ^A	5.5 ± 1.6 ^A
Fluid reabsorption (μl/min)	WT	391 ± 24	386 ± 22	416 ± 31	398 ± 29	372 ± 40	336 ± 40
	KO	442 ± 57	462 ± 60	397 ± 63	421 ± 36	422 ± 32	404 ± 19

See Table 1 for abbreviations. WT, $n = 5$; KO, uroguanylin knockout, $n = 5$. Values are mean ± SEM. ^A $P < 0.05$ compared with control value in the same group. ^B $P < 0.05$ compared with WT for pooled control data from enteral- and i.v.-loaded animals. ^C $P < 0.05$ compared with the corresponding time point in the WT group.



ing enteral NaCl load (see Table 1). Extrapolating over several hours, it can be predicted that most of the NaCl load given to the WT animals would have been excreted within about 3 hours, but in the uroguanylin knockout animals, the observed rate of Na⁺ excretion would require over 6 hours to fully eliminate the load. In contrast to the observations in the original reports from Carey et al., in the present experiment the intravenous load was excreted much faster than the enteral load (35, 36). As shown in Figure 7, sodium excretion increased dramatically within the first 20 minutes of i.v. NaCl administration, whereas the increase immediately after enteral loading was more subtle. The conditions of the present experiment were quite different however, in that the NaCl load was substantially larger (10 times), and it was delivered in a much larger volume of fluid. Thus, the present paradigm, providing NaCl in 1 ml of water (approximately 3% of body weight), would be expected to have sizable BP and hemodynamic consequences, whereas the volume delivered in Carey's experiments was minimal (approximately 0.3%) and would likely have a negligible influence on renal hemodynamics.

It is relevant to note that the natriuretic response to intravenous volume loading is believed to be largely dependent on the actions of atrial natriuretic peptide, which acts through the guanylate cyclase A (GC-A) receptor in the kidney (39). Furthermore, it was recently shown that two distinct signaling pathways may participate in the proximal tubular responses to uroguanylin: one involving GC-C and the other involving a cGMP-independent, pertussis toxin-sensitive G protein (40). Consistent with previous studies using semiquantitative and real-time RT-PCR (10, 41), we

Figure 7

Renal clearance measurements from *Ugn*^{+/+} and *Ugn*^{-/-} given either enteral NaCl load or intravenous NaCl load; total amount of Na⁺ was 300 μEq delivered in 1 ml of fluid over 1 to 2 minutes. (a) Filtered load of Na⁺ (FL Na⁺) before (time 0) and after NaCl administration. (b) Cumulative Na⁺ excretion (U_{Na⁺}V) before and after NaCl administration. Number of animals in each group is shown in parentheses. **P* < 0.05 compared with control value (time 0) in the same group; †*P* < 0.05 compared with the corresponding time point in the *Ugn*^{+/+} group.

confirmed the renal expression of GC-C mRNA by RT-PCR analysis in the present study (Figure 3), suggesting that the receptor is present in the kidney, but at levels undetectable by Northern analysis. The observed increase in renal GC-C mRNA in *Ugn*^{-/-} mice might be consistent with physiologic upregulation of this receptor in response to loss of uroguanylin.

In addition to its proposed endocrine/paracrine/autocrine role in mediating NaCl excretion from the kidney, uroguanylin is thought to participate in the local regulation of salt and water transport within the GI tract itself (see refs. 5 and 38 for reviews). Within the intestine, guanylin peptides interact with the GC-C receptor expressed in most intestinal epithelial cells, and the resultant production of cGMP leads to increased Cl⁻ secretion in part through PKG II-mediated phosphorylation of cystic fibrosis transmembrane conductance regulator, as well as inhibition of Na⁺ and water absorption across the enterocyte (42). It is therefore possible that uroguanylin deficiency might result in alterations in the rate of water and electrolyte absorption from the GI tract that may, in turn, ultimately influence the rate of NaCl excretion from the kidney following an enteral NaCl load, independent from any intestine-to-kidney signaling events per se. However, since uroguanylin is considered to be a

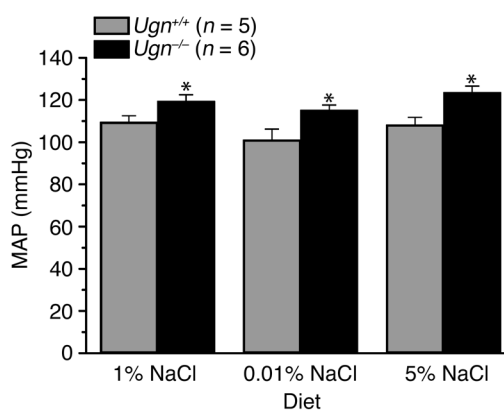


Figure 8

Telemetric measurements of mean arterial pressure (MAP) in *Ugn*^{+/+} and *Ugn*^{-/-} mice that were sequentially fed a normal (1%), low (0.01%), and high (5%) NaCl diet for at least 3 days. Following surgical implantation, animals were allowed to recover for 5 to 7 days, and diets were administered in the order presented. BP was monitored continuously and the data shown represent 2-hour averages taken between 4:00 am and 6:00 am on the third day of each diet while the animals were resting quietly. **P* < 0.02 compared with *Ugn*^{+/+}.

potent secretagogue, one would expect that uroguanylin deficiency would, if anything, result in accelerated rates of net salt and water absorption from the intestine. In fact, in Ussing chamber studies chambers, we found that net Na⁺/H⁺ exchanger-mediated (NHE-mediated) Na⁺ absorption, as well as total tissue conductance, was not different in *Ugn*^{-/-} animals compared with *Ugn*^{+/+}, and that electrogenic anion secretion (indicated by short-circuit current) was essentially abolished in the knockout animals (Figure 4). Thus, it seems unlikely that the observed decrement in Na⁺ excretion following enteral NaCl administration in UGN-KO mice could be accounted for by decreased intestinal absorption of the salt load.

Telemetric measurement of arterial pressure revealed that uroguanylin deficiency results in a significant elevation of BP, but interestingly, does not influence short term salt-sensitivity. Regardless of the salt content of the diet, BP under resting conditions was consistently 10–15 mmHg higher in the uroguanylin knockout animals compared with WT. To explore the possibility that there might be a transient elevation in BP due to abnormal Na⁺ retention when salt intake was suddenly increased (0.01% to 5% NaCl diet), we analyzed BP continuously over the 24-hour period following the switch to the high-salt diet. We found that BP increased slightly (but not significantly) in both WT and knockout mice, and there was no indication that the change was different between the two genotypes. Although the observation that the BP effects of uroguanylin deficiency are not salt sensitive is somewhat puzzling, similar effects have been documented in GC-A knockout mice (39). Additionally, it is possible that longer-term treatment with low- and high-salt diets may reveal a greater difference in salt sensitivity between the two genotypes. Finally, although the BP differences between genotypes did not persist in anesthetized animals prepared for clearance measurements (Tables 1 and 2), it is important to note that barbiturate anesthesia can often mask BP differences between groups.

The phenotype of *Ugn*^{-/-} animals is also remarkable for the apparent decrease in guanylin protein in the intestine. This is not due to a structural alteration in the guanylin gene. A potential explanation may be feedback downregulation of guanylin resulting from the loss of uroguanylin expression. However, no such decrease in uroguanylin expression was seen in guanylin gene-targeted animals (23). Alternatively, we have considered that the change in guanylin expression may be a result of the alteration in the immediate flanking sequence of uroguanylin caused by the targeting construct. Since previous experiments have indicated that important controlling elements for guanylin gene expression remain to be discerned (43), it is possible that the promoter sequence of uroguanylin, which is highly homologous to guanylin and is located in close proximity, may have important regulatory features for guanylin gene expression.

Because the *Ugn*^{-/-} mouse has diminished expression of guanylin, we cannot exclude the possibility that guanylin is also an intestinal natriuretic peptide. It is possible, therefore, that our observed effects might be attributable to the deficiency in guanylin as well as or even instead of uroguanylin. It is nonetheless important that major effects in renal sodium handling and BP are observed as a result of changes in the expression of members of the guanylin family of peptides. Furthermore, experiments are ongoing to evaluate guanylin knockout mice, and evidence from metabolic cage experiments suggests that *Ugn*^{-/-} but not guanylin^{-/-} mice demonstrate impaired enteral salt excretion on a high-salt diet (44). In addition, uroguanylin is more potent than guanylin as a natriuretic agent and is normally present in much higher concentrations in the proximal small intestine. Thus we believe that the effects observed on excretion of an enteric salt load are more likely due to loss of uroguanylin.

In conclusion, it is likely that there are a number of novel functions for the uroguanylin ligand family of intestinal peptides. In addition to its role as an intestinal secretagogue, uroguanylin acts as a critical renal regulator of dietary salt intake, that is, an intestinal natriuretic peptide. This fundamental physiologic observation has broad implications for therapeutic control of intravascular volume and overall electrolyte and volume homeostasis.

Acknowledgments

This work was supported by National Institutes of Health grants DK57552 and DK 47318. We thank S.A. Wovk for technical assistance.

- Currie, M., et al. 1992. Guanylin: an endogenous activator of intestinal guanylate cyclase. *Proc. Natl. Acad. Sci. U. S. A.* **89**:947–951.
- Hamra, F.K., et al. 1993. Uroguanylin: structure and activity of a second endogenous peptide that stimulates intestinal guanylate cyclase. *Proc. Natl. Acad. Sci. U. S. A.* **90**:10464–10468.
- Forte, L.R., Fan, X., and Hamra, F.K. 1996. Salt and water homeostasis: uroguanylin is a circulating peptide hormone with natriuretic activity. *Am. J. Kidney Dis.* **28**:296–304.
- Forte, L.R., London, R.M., Freeman, R.H., and Krause, W.J. 2000. Guanylin peptides: renal actions mediated by cyclic GMP. *Am. J. Physiol. Renal Physiol.* **278**:F180–F191.
- Forte, L.R., London, R.M., Krause, W.J., and Freeman, R.H. 2000. Mechanisms of guanylin action via cyclic GMP in the kidney. *Annu. Rev. Physiol.* **62**:673–695.
- Hess, R., et al. 1995. GCAP-II: isolation and characterization of the circulating form of human uroguanylin. *FEBS Lett.* **374**:34–38.
- Kuhn, M., et al. 1993. The circulating bioactive form of human guanylin is a high molecular weight peptide (10.3 kDa). *FEBS Lett.* **318**:205–209.
- Martin, S., Adermann, K., Forssmann, W.G., and Kuhn, M. 1999. Regulated, side-directed secretion of proguanylin from isolated rat colonic mucosa. *Endocrinology.* **140**:5022–5029.
- Carrithers, S.L., Jackson, B.A., Cai, W.Y., Greenberg, R.N., and Ott, C.E. 2002. Site-specific effects of dietary salt intake on guanylin and uroguanylin mRNA expression in rat intestine. *Regul. Pept.* **107**:87–95.
- Potthast, R., et al. 2001. High salt intake increases uroguanylin expression in mouse kidney. *Endocrinology.* **142**:3087–3097.
- Kinoshita, H., et al. 1997. Urine and plasma levels of uroguanylin and its molecular forms in renal diseases. *Kidney Int.* **52**:1028–1034.
- Kinoshita, H., et al. 1999. Plasma and urine levels of uroguanylin, a new natriuretic peptide, in nephrotic syndrome. *Nephron.* **81**:160–164.
- Carrithers, S.L., Eber, S.L., Forte, L.R., and Greenberg, R.N. 2000. Increased urinary excretion of uroguanylin in patients with congestive heart failure. *Am. J. Physiol. Heart Circ. Physiol.* **278**:H538–H547.
- Nakazato, M., et al. 1998. Tissue distribution, cellular source, and

- structural analysis of rat immunoreactive uroguanylin. *Endocrinology*. **139**:5247–5254.
15. Whitaker, T.L., Witte, D.P., Scott, M.C., and Cohen, M.B. 1997. Uroguanylin and guanylin: distinct but overlapping patterns of messenger RNA expression in mouse intestine. *Gastroenterology*. **113**:1000–1006.
 16. Steinbrecher, K.A., Mann, E.A., Giannella, R.A., and Cohen, M.B. 2001. Increases in guanylin and uroguanylin in a mouse model of osmotic diarrhea are guanylate cyclase C-independent. *Gastroenterology*. **121**:1191–1202.
 17. Fonteles, M.C., Greenberg, R.N., Monteiro, H.S., Currie, M.G., and Forte, L.R. 1998. Natriuretic and kaliuretic activities of guanylin and uroguanylin in the isolated perfused rat kidney. *Am. J. Physiol.* **275**:F191–F197.
 18. Greenberg, R.N., et al. 1997. Comparison of effects of uroguanylin, guanylin, and *Escherichia coli* heat-stable enterotoxin STa in mouse intestine and kidney: evidence that uroguanylin is an intestinal natriuretic hormone. *J. Invest. Med.* **45**:276–282.
 19. Fukae, H., et al. 2002. Changes in urinary levels and renal expression of uroguanylin on low or high salt diets in rats. *Nephron*. **92**:373–378.
 20. Fujimoto, S., et al. 2000. Immunohistochemical localization of uroguanylin in the human kidney. *Nephron*. **84**:88–89.
 21. Yuge, S., Inoue, K., Hyodo, S., and Takei, Y. 2003. A novel guanylin family (guanylin, uroguanylin, and renoguanylin) in eels: possible osmoregulatory hormones in intestine and kidney. *J. Biol. Chem.* **278**:22726–22733.
 22. Whitaker, T.L., et al. 1997. The uroguanylin gene (Guca1b) is linked to guanylin (Guca2) on mouse chromosome 4. *Genomics*. **45**:348–354.
 23. Steinbrecher, K.A., Wowk, S.A., Rudolph, J.A., Witte, D.P., and Cohen, M.B. 2002. Targeted inactivation of the mouse guanylin gene results in altered dynamics of colonic epithelial proliferation. *Am. J. Pathol.* **161**:2169–2178.
 24. Swenson, E.S., Mann, E.A., Jump, M.L., Witte, D.P., and Giannella, R.A. 1996. The guanylin/STa receptor is expressed in crypts and apical epithelium throughout the mouse intestine. *Biochem. Biophys. Res. Commun.* **225**:1009–1014.
 25. Perkins, A., Goy, M.F., and Li, Z. 1997. Uroguanylin is expressed by enterochromaffin cells in the rat gastrointestinal tract. *Gastroenterology*. **113**:1007–1014.
 26. Li, Z., Taylor-Blake, B., Light, A.R., and Goy, M.F. 1995. Guanylin, an endogenous ligand for C-type guanylate cyclase, is produced by goblet cells in the rat intestine. *Gastroenterology*. **109**:1863–1875.
 27. Balint, J.P., Kosiba, J.L., and Cohen, M.B. 1997. The heat-stable enterotoxin-guanylin receptor is expressed in rat hepatocytes and in a rat hepatoma (H-35) cell line. *J. Recept. Signal Transduct. Res.* **17**:609–630.
 28. Clarke, L.L., et al. 1992. Defective epithelial chloride transport in a gene-targeted mouse model of cystic fibrosis. *Science*. **257**:1125–1128.
 29. Clarke, L.L., and Argenzio, R.A. 1990. NaCl transport across equine proximal colon and the effect of endogenous prostanoids. *Am. J. Physiol.* **259**:G62–G69.
 30. Gawenis, L.R., et al. 2002. Intestinal NaCl transport in NHE2 and NHE3 knockout mice. *Am. J. Physiol. Gastrointest. Liver Physiol.* **282**:G776–G784.
 31. Musch, M.W., et al. 2002. T cell activation causes diarrhea by increasing intestinal permeability and inhibiting epithelial Na⁺/K⁺-ATPase. *J. Clin. Invest.* **110**:1739–1747. doi:10.1172/JCI200215695.
 32. Lorenz, J.N., and Gruenstein, E. 1999. A simple, nonradioactive method for evaluating single-nephron filtration rate using FITC-inulin. *Am. J. Physiol. Renal Physiol.* **276**:F172–F177.
 33. Butz, G.M., and Davisson, R.L. 2001. Long-term telemetric measurement of cardiovascular parameters in awake mice: a physiological genomics tool. *Physiol. Genomics*. **5**:89–97.
 34. Sciaky, D., et al. 1995. Mapping of guanylin to murine chromosome 4 and human chromosome 1p34-p35. *Genomics*. **26**:427–429.
 35. Lennane, R.J., Carey, R.M., Goodwin, T.J., and Peart, W.S. 1975. A comparison of natriuresis after oral and intravenous sodium loading in sodium-depleted man: evidence for a gastrointestinal or portal monitor of sodium intake. *Clin. Sci. Mol. Med.* **49**:437–440.
 36. Carey, R.M., Smith, J.R., and Ortt, E.M. 1976. Gastrointestinal control of sodium excretion in sodium-depleted conscious rabbits. *Am. J. Physiol.* **230**:1504–1508.
 37. Krause, W.J., et al. 1997. Guanylyl cyclase receptors and guanylin-like peptides in reptilian intestine. *Gen. Comp. Endocrinol.* **107**:229–239.
 38. Nakazato, M. 2001. Guanylin family: new intestinal peptides regulating electrolyte and water homeostasis. *J. Gastroenterol.* **36**:219–225.
 39. Dubois, S.K., Kishimoto, I., Lillis, T.O., and Garbers, D.L. 2000. A genetic model defines the importance of the atrial natriuretic peptide receptor (guanylyl cyclase-A) in the regulation of kidney function. *Proc. Natl. Acad. Sci. U. S. A.* **97**:4369–4373.
 40. Sindice, A., et al. 2002. Guanylin, uroguanylin, and heat-stable enterotoxin activate guanylate cyclase C and/or a pertussis toxin-sensitive G protein in human proximal tubule cells. *J. Biol. Chem.* **277**:17758–17764.
 41. Carrithers, S.L., et al. 2000. Guanylyl cyclase-C receptor mRNA distribution along the rat nephron. *Regul. Pept.* **95**:65–74.
 42. Vaandrager, A.B., et al. 2000. Differential role of cyclic GMP-dependent protein kinase II in ion transport in murine small intestine and colon. *Gastroenterology*. **118**:108–114.
 43. Goday, P.S., and Cohen, M.B. 2001. The intronic sequence of the mouse guanylin gene directs high ileal reporter gene transcription in transgenic mice. *Gastroenterology*. **120**:A304. (Abstr.)
 44. Elitsur, N., et al. 2003. Uroguanylin but not guanylin knockout mice have diminished excretion of sodium on a high salt diet. *Gastroenterology*. **124**:A140. (Abstr.)